

## PEEK HIGH PERFORMANCE FUSED DEPOSITION MODELING MANUFACTURING WITH LASER IN-SITU HEAT TREATMENT

M Luo\*, X Tian\*, J Shang\*, W Zhu\*, D Li\*

\* State Key Laboratory of Manufacturing Systems Engineering, Xi'an Jiaotong University, 710049, China

### Abstract

Because of the thermal resistance, high mechanical properties, biocompatibility, PEEK have increasingly extended their application in medicals, aircraft, industrial fields and so on. In FDM, a low crystallinity can be got to limit volume contraction to avoid weak interlaminar bonding, which results in the conflict between high interlaminar bonding and crystallinity. In this study, a CO<sub>2</sub> laser device was adopted to improve both the interlaminar shear strength and the crystallinity of PEEK part synchronously in FDM. A series of test was then successively implemented. And after the observation and the analysis of the results, an obvious improvement was got that its interlaminar shear strength could improve over 45%, while its crystallinity could improve over double times for PEEK. Additionally, the process suggests a much potential in developing the gradient distribution of the crystallinity or stiffness in multi-function integration manufacturing for PEEK-like semi-crystalline materials.

### Introduction

Because of their advantages of thermal resistance, desirable mechanical properties, and biocompatibility [1–3], semicrystalline thermoplastic polymer, such as poly(ether ether ketone) (PEEK), have been used as replacements for metals in many different applications [4–7]. These excellent performance characteristics of semicrystalline polymers are closely related to their semicrystalline forms, which are significantly influenced by the thermal cycles in the forming process [8–12]. Many industrial techniques have been used to manufacture products made of semicrystalline materials, such as injection moulding, pressing, and sintering, as well as emerging additive manufacturing processes [4,13,14]. Compared to traditional manufacturing, additive manufacturing techniques such as SLS and FDM have provided an innovative way to simplify processing and realize the manufacture of complex structural parts of high-performance polymers. In order to reshape the filiform raw materials, FDM has been reported to undergo a typical heating and cooling procedure [15–17], which influences the product's crystallinity and final properties, especially for semicrystalline materials [18].

In the conventional FDM process for semicrystalline materials, two problems exist simultaneously. First, the bonding strength of two adjacent layers is too low [19–21]. And secondly, it's complicated to improve the part's crystallinity. In order to improve the external interlayer bonding, most research adapted the rapid cooling to limit the big volume contraction, which results in the internal insufficient crystallization [14,22–23]. Therefore, the two phenomena affect each other. Aimed on solving the problems, a series of post heat treatments such as annealing have also been adapted after the rapid cooling printing to improve the part's crystallinity again, which leads to a more complex process during printing. Also, the post treatment can only help get the part with approximate crystallinity. Besides, in some cases, controlling the crystallization different in different region when printing a part could be very necessary, which asks for a more effective and simple method to realize these. Thus, a further research is required and introduced in this paper.

Therefore, a laser in-situ heat treatment process for PEEK-like semicrystalline materials has been proposed to solve and optimize the two problems. An optimized FDM system was set up with a CO<sub>2</sub> laser device. PEEK samples were prepared with and without laser assistance to compare with each other, and their interlayer shear strength and crystallinity were compared and analysed below.

## Equipment, Materials, and Methods

### Equipment and Materials

A CO<sub>2</sub> laser device with a maximum power of approximately 40 W and wavelength of approximately 10.6  $\mu\text{m}$  is integrated into the FDM printer. Fig. 1a has shown the laser reflection path in detail and then finally focused on the part through the laser focusing lens. The real equipment has shown as Fig. 1e. A series of steps were utilized here to realize the printing as follows.

1) The PEEK filaments used here were prepared from reprocessing from PEEK pellets (450 G, VICTREX Corp., UK).

2) A traditional 3-degree FDM printer system was chosen to combine the CO<sub>2</sub> laser device with maximum power of 40W and wavelength 10600 nm.

3) Four mirrors were set up to construct an effective optical path to make sure the laser can reflect one by one and in the end focus on the front of the printing nozzle shown in Fig. 1a.

4) Design the sample and test the performance.

The glass transition temperature ( $T_g$ ) of the PEEK is approximately 143 °C, its melting temperature ( $T_m$ ) is approximately 343 °C, and its degradation temperature ( $T_d$ ) is approximately 420 °C. In this study, the basic process parameters, including the printing speed, layer thickness, nozzle diameter, and heating temperature for fusion of the PEEK are maintained at 6 mm/s, 0.2 mm, 0.4 mm, and 410 °C, respectively.

### Test of Temperature

To study the relationship among the surface temperature, interlayer shear strength, crystallinity, and laser parameters, a laser was used at 5%, 10%, 15%, 20% of its 40 W maximum power. And the temperature was then measured by an infrared thermal imager (E50, FLIR Systems AB Corp., Sweden). The thermal image has shown in Fig. 1b.

### Sample design

A printing sample was designed and printed as shown in Fig. 1c. The nozzle follows the arrows moving in a circular path in each layer. During printing, the laser is controlled to be powered on red side and off on the other sides; thus, the laser-on side can always receive the in-situ laser heat treatment, whereas the other sides receive no extra heating treatment. As Fig. 1c shows, the outer length and width are respectively 50mm and 30mm, while the inner length and width are respectively 30mm and 10mm. The thickness of the sample is about 2mm. After printing, a pair of standard samples can be obtained by cutting the longest opposite sides of the rectangular annular sample seen in Fig. 1d. The standard sample's length, width and thickness are respectively approximately 20±1 mm, 10±0.2 mm and 2±0.2 mm.

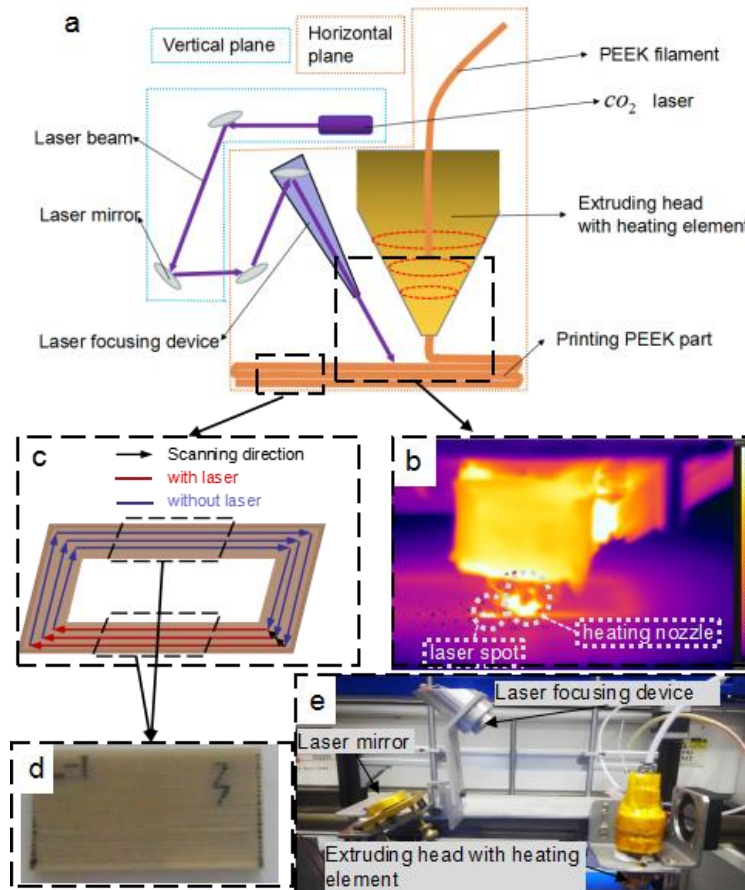


Fig.1 Printer system and designed sample. Diagram of printer system (a), temperature distribution obtained by an infrared thermal imager (b), designed annular rectangular sample (c), standard sample to test (d), and real printer system (e).

### Short-beam test

According to the standard for interlayer shear strength testing by the short-beam method (JC/T 773-2010 in China), a short-beam-shaped PEEK part is needed to implement a three-point bending test in a universal testing machine (PLD-5kN, LETRY Corp., China). The pressure head diameter, span, and speed of pressurisation are approximately  $5 \pm 0.2$  mm, 10 mm, and  $1 \pm 0.2$  mm/min, respectively. As shown in Fig.1c, after the annular rectangular part is printed, standard testing samples with a length of approximately 20 mm are cut from the long side. The width and thickness of the samples are approximately 10 and 2 mm, respectively. After the experiment, using the premeasured width ( $b$ /mm) and thickness ( $h$ /mm) and the yield force ( $F$ /N) obtained in the experiment, the interlayer shear strength ( $\tau_m$ /MPa) can be calculated as

$$\tau_m = 3F/4bh \quad (1)$$

### DSC test to assess crystallinity

The degree of crystallinity of the samples was measured using a standard differential scanning calorimeter (DSC1, Mettler Toledo Corp., Switzerland). All samples were heated at a rate of  $10^\circ\text{C}/\text{min}$  to a temperature of  $400^\circ\text{C}$ . The mass fraction of the crystalline region is then given by

$$\chi_c = (\Delta H_f + \Delta H_c) / \Delta H_f^0 \quad (2)$$

where  $\Delta H_f$  and  $\Delta H_c$  represent the measured values of the melting enthalpy and the cold crystallization exothermal energy, respectively.  $\Delta H_f^0$  is the melting enthalpy of PEEK with 100% crystallinity and equals 130 J/g [24].

## Results and Discussion

### Relationship between preheating temperature and laser power

During printing, the thermal camera was used to capture the temperature distribution photos. The temperature in different points could then be processed with the software of FLIR Tools (FLIR Tools, FLIR Systems AB Corp., Sweden) as same as Fig.1b. The obvious laser point and the interlayer bonding point could be seen in the photo, while the photo with no laser was also captured during printing to compare to prove that the laser is the only factor to influence the temperature's improvement.

The relationship between the laser power and heating efficiency was then established. The measured temperature is shown in Fig.2. As the laser power increases, the temperatures of the laser point and interlayer bonding point marked in Fig. 1a are both increased.

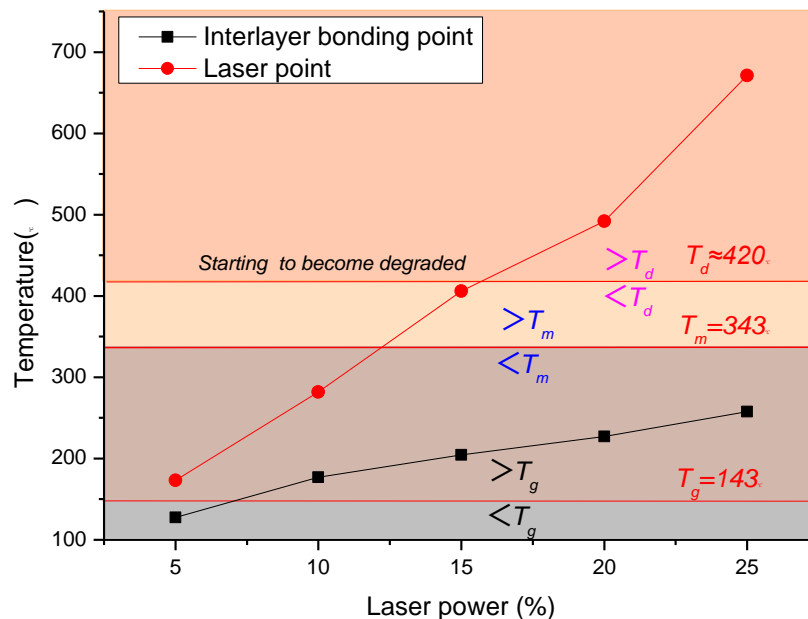


Fig.2 Temperature of interlayer bonding point and laser point at different laser powers.

### Effect of laser preheating temperature on crystallinity

As talked before, the cooling condition mainly influences the crystallinity. The laser used in the process reheat the printed PEEK part to help improve the crystallinity. However, different temperatures implemented during printing can result in different crystallinity. Therefore, a DSC analysis of the printed samples was performed. Before laser treatment, the cold crystallization peak and crystal melting peak both theoretically exist in the DSC curve shown in Fig.3. However, the laser treatment aims to eliminate the cold crystallization peak in the DSC curves by supporting the ongoing crystallization of the PEEK samples during printing. As shown in Fig.3, as the temperature increases, the crystallinity of the samples shows a corresponding increase. Without the laser, the crystallinity of PEEK is just retained at powers of less than 15%. With laser assistance, the much higher temperature improves the crystallinity to 34.5%, which approaches PEEK's typical crystallinity of 35%.

Because PEEK is a semicrystalline thermoplastic material, its mechanical properties, including the elastic modulus and yield strength, are obviously influenced by the degree of crystallinity. Related research has been reported previously [1,14,25,26].

Except of the applied ambient heat treatment control [14,17] and post heat treatment control [14,23], the laser in-situ heat treatment process affects the cooling conditions in region, thus to control crystallinity. Therefore,

to realize crystallinity control, adjusting the corresponding laser parameters such as the laser power to change the temperature is a simple way.

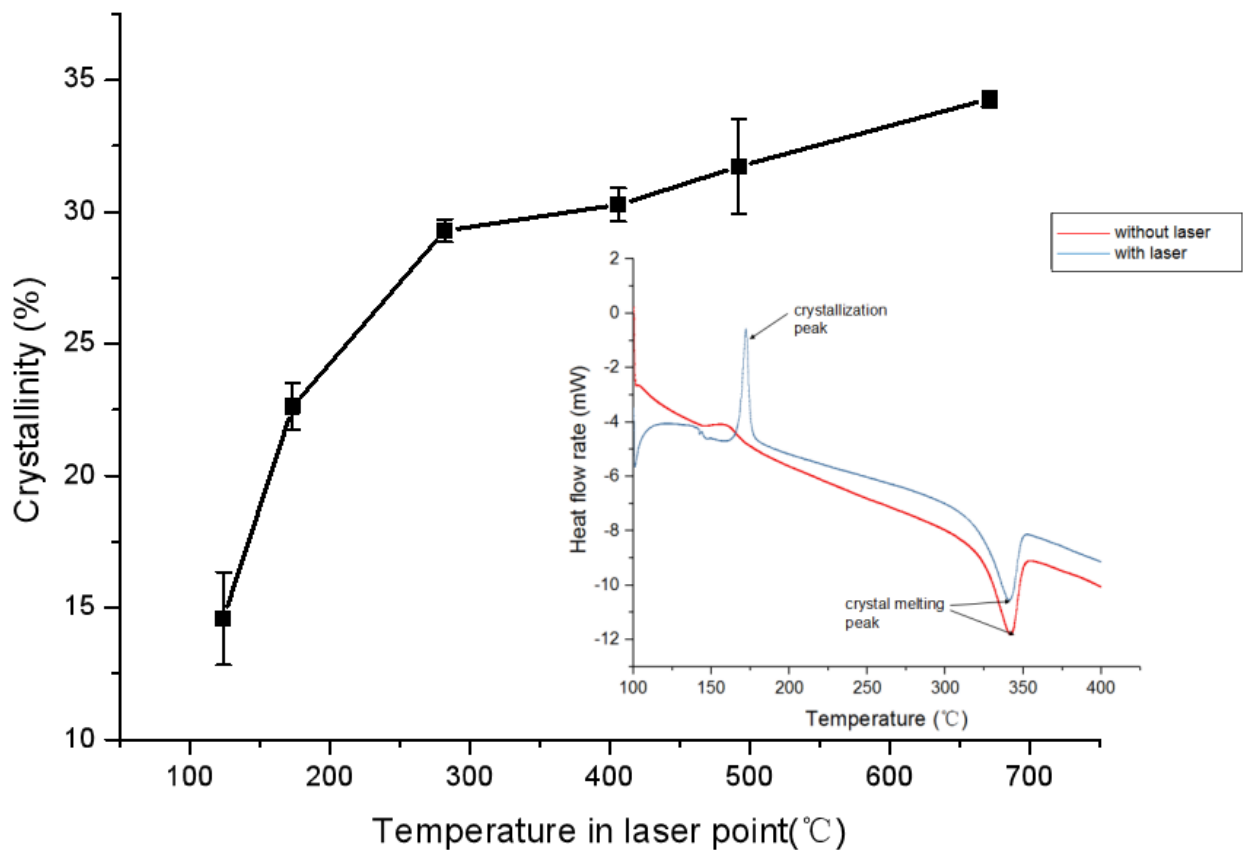


Fig.3 Controllable crystallization of PEEK specimens with different laser point temperatures.

### Effect of laser preheating temperature on interlayer bonding

The interlayer shear strength was measured to assess the interlayer bonding effect. The force–displacement curve is obtained by performing a three-point bending test on a universal testing machine, and then the stress–strain curve is obtained. The measurement data for the interlayer shear strength are shown in Fig.4. When the temperature of the laser point is less than  $T_g$ , the process provides little improvement in the interlayer bonding. Further, as the temperature increases above  $T_g$ , the interlayer shear strength obviously improves. The optimal bonding performance appears at a laser power of 15%, and the interlayer shear strength can improve by more than 45%, as shown in Fig.4, which strongly indicates the potential of high-performance additive manufacturing using PEEK-like semicrystalline thermoplastics.

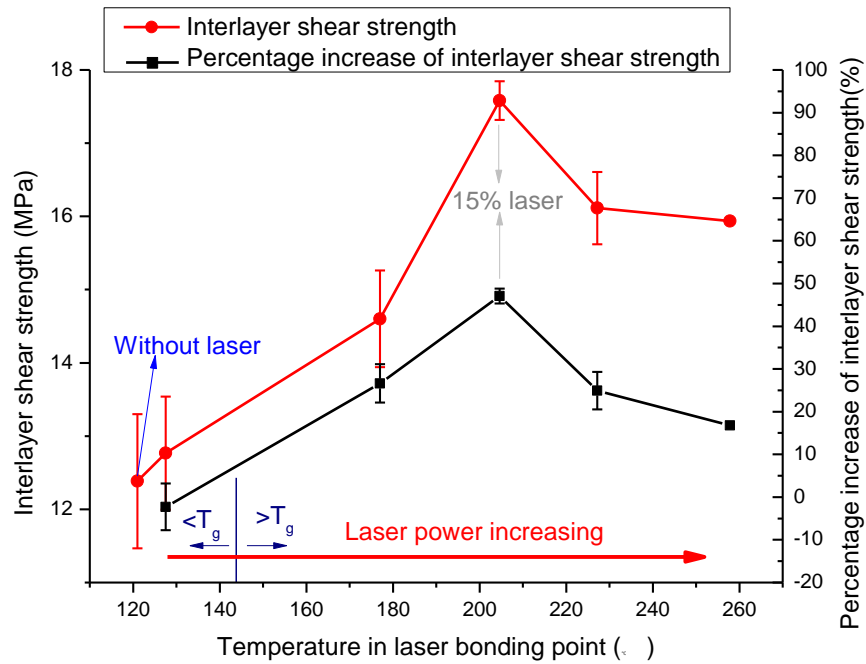


Fig.4 Interlayer shear strength and percentage increase of interlayer shear strength with different interlayer bonding point temperatures.

## Further Discussion

### Interlayer bonding

There is reportedly a critical temperature that affects the interpenetration of molecular chains across a bonding interface [27]. Further,  $T_g$  has been proven to be the critical temperature at which interface disappearance and bond development in thermoplastic materials are facilitated during FDM manufacturing [19,28]. In recent years, there have been many studies on improving the interlayer strength of amorphous materials such as acrylonitrile-butadiene-styrene (ABS) and polylactic acid [19-21], and the flexural strength of extruded ABS material components can be increased to a maximum of 95% by in-situ heating. Unlike the case for amorphous materials, delamination is always obvious in semicrystalline materials [4], and it is usually the primary form of failure in PEEK-like semicrystalline materials in a bending process.

The laser acts as a heat source to improve interlayer bonding in region at two levels. Macroscopically, the laser heats the previous layer to form a regional molten bath that adaptively bonds with the melting printing layer as it decreases in volume. Microscopically, the laser helps heat the bonding point in the previous layer to above  $T_g$  to effectively improve the interpenetration of the molecular chain ends [27]. By systematically analysing the Fig.4, we find that the interlayer bonding in the laser power of 5% has no obvious improvement because of lower temperature than  $T_g$ , and the laser power point of 15% has the most excellent bonding effect, which shows declination because of degradation when over 15%. A related discussion has been reported previously [29]. Therefore, maintaining a suitable heating temperature by laser power control could easily facilitate optimal interlayer bonding.

### Simultaneous effect of laser on interlayer bonding and crystallinity

As an effective process, laser-assisted heat treatment has been widely used in tape placement [30-33]. By combining laser preheating and post-hot-rolling processes, the tape placement process can firmly bond a metal laminate and a plastic tape. The research reported here is successfully inspired by the concept of tape placement, where the laser-assisted heat treatment process is used to preheat the interlayer bonding points to a temperature exceeding  $T_g$ , thereby greatly enhancing the cross-linking and interpenetration of molecular chains at the interface.

At the same time, for semicrystalline materials, the crystallinity can be controlled by adjusting the laser power to achieve controllability of the material modulus and rigidity of the components. Therefore, this is the first time that a simple process has been used to improve the interlayer shear strength and realize regional controllability of the crystallinity simultaneously for PEEK-like semicrystalline materials.

### **Conclusion**

The interlayer shear strength and crystallinity of PEEK-like semicrystalline materials usually have conflicting manufacturing requirements, so most processes optimize one parameter at the expense of the other. In this paper, a laser in-situ heat treatment FDM process for PEEK has been demonstrated to effectively improve both the interlayer shear strength and the crystallinity simultaneously. The interlayer shear strength can be improved by more than 45%; further, the crystallinity was more than two times higher than that obtained without the laser treatment and approached to the typical crystallinity of 35%. Furthermore, the mapping relationship between various laser parameters, temperatures and the performance of the produced components has been successfully established to help realize controllability of the interlayer shear strength and local control of the crystallinity by adjusting the laser power within the effective range.

### **Acknowledgements**

This work was supported by the National Natural Science Foundation of China (NO. 51575430), National Key Research and Development Program of China (NO.2017YFB1103401, 2016YFB1100902).

### **References**

- 1.Kurtz S M, Devine J N. PEEK biomaterials in trauma, orthopedic, and spinal implants.[J]. *Biomaterials*, 2007, 28(32):4845.
- 2.Toth J M, Wang M, Estes B T, Scifert J L, Seim HB 3rd, Turner AS. Polyetheretherketone as a biomaterial for spinal applications[J]. *Biomaterials*, 2006, 27(3):324.
- 3.Williams D F, Mcnamara A, Turner R M. Potential of polyetheretherketone (PEEK) and carbon-fibre-reinforced PEEK in medical applications[J]. *Journal of Materials Science Letters*, 1987, 6(2):188-190.
- 4.Vaezi M, Yang S. Extrusion-based additive manufacturing of PEEK for biomedical applications[J]. *Virtual & Physical Prototyping*, 2015, 10(3):123-135.
- 5.Garcia-Gonzalez D, Rusinek A, Jankowiak T, Arias A. Mechanical impact behavior of polyether-ether-ketone (PEEK)[J]. *Composite Structures*, 2015, 124(4):88-99.
- 6.Lovald S, Kurtz S M. Chapter 15 – Applications of Polyetheretherketone in Trauma, Arthroscopy, and Cranial Defect Repair[J]. *Peek Biomaterials Handbook*, 2012:243-260.
- 7.Kurtz S M. Chemical and Radiation Stability of PEEK[M]// *PEEK Biomaterials Handbook*. Elsevier Inc. 2012:75-79.
- 8.Waddon A J, Hill M J, Keller A, Blundell D J. On the crystal texture of linear polyaryls (PEEK, PEK and PPS)[J]. *Journal of Materials Science*, 1987, 22(5):1773-1784.
- 9.Hamdan S, Swallowe G M. Crystallinity in PEEK and PEK after mechanical testing and its dependence on strain rate and temperature[J]. *Journal of Polymer Science Part B Polymer Physics*, 2015, 34(4):699-705.
- 10.Talbott M F, Springer G S, Berglund L A. The Effects of Crystallinity on the Mechanical Properties of PEEK Polymer and Graphite Fiber Reinforced PEEK[J]. *Journal of Composite Materials*, 1987, 21(11):1056-1081.
- 11.Zhang G, Schlarb A K. Correlation of the tribological behaviors with the mechanical properties of poly-ether-ether-ketones (PEEKs) with different molecular weights and their fiber filled composites[J]. *Wear*, 2009, 266(1):337-344.
- 12.Liu T, Mo Z, Wang S, Zhang H. Nonisothermal melt and cold crystallization kinetics of poly(aryl ether ether ketone ketone)[J]. *Polymer Engineering & Science*, 1997, 37(3):568–575.
- 13.Osswald T A. Materials. In: *International plastics handbook: the resource for plastics engineers*[M]. Hanser Gardner Pubns, 2006, pp.613-621.

14. Yang C, Tian X, Li D, Cao Y, Zhao F, Shi C. Influence of thermal processing conditions in 3D printing on the crystallinity and mechanical properties of PEEK material[J]. *Journal of Materials Processing Technology*, 2017, 248:1-7.
15. Valentan B, Kadivnik Z, Brajljeh T, Anderson A, Drstvenšek I. Processing poly(ether etherketone) on a 3d printer for thermoplastic modelling[J]. *Materiali in Tehnologije*, 2013, 47(6):715-721.
16. Gibson I, Rosen D W, Stucker B. *Additive Manufacturing Technologies – Rapid Prototyping to Direct Digital Manufacturing*[M]. Springer US, 2010.
17. Wu W Z, Geng P, Zhao J, Zhang Y, Rosen D W, Zhang H B. Manufacture and thermal deformation analysis of semicrystalline polymer polyether ether ketone by 3D printing[J]. *Material Research Innovations*, 2015, 18(S5):S12-S16.
18. Zalaznik M, Kalin M, Novak S. Influence of the processing temperature on the tribological and mechanical properties of poly-ether-ether-ketone (PEEK) polymer[J]. *Tribology International*, 2016, 94:92-97.
19. Ravi A K. A Study on an In-Process Laser Localized Pre-Deposition Heating Approach to Reducing FDM Part Anisotropy[D]. ARIZONA STATE UNIVERSITY, 2016.
20. Kishore V, Ajinjeru C, Nycz A, Post B, Lindahl J, Kunc V, Duty C. Infrared preheating to improve interlayer strength of big area additive manufacturing (BAAM) components[J]. *Additive Manufacturing*, 2017, 14: 7-12.
21. Sun Q, Rizvi G M, Bellehumeur C T, P Gu. Effect of processing conditions on the bonding quality of FDM polymer filaments[J]. *Rapid Prototyping Journal*, 2008, 14(2):72-80.
22. Gomes A C D O, Soares B G, Oliveira M G, Machado J C, Windmöller D, Paranhos C M . Characterization of crystalline structure and free volume of polyamide 6/nitrile rubber elastomer thermoplastic vulcanizates: Effect of the processing additives[J]. *Journal of Applied Polymer Science*, 2017, 134(48):45576.
23. Cebe P, Hong S D. Crystallization behaviour of poly(ether-ether-ketone)[J]. *Polymer*, 1986, 27(8):1183-1192.
24. Blundell D J, Osborn B N. The morphology of poly(aryl-ether-ether-ketone)[J]. *Polymer*, 1983, 24(8):953-958.
25. Chivers R A, Moore D R, Chivers R A, Moore D R. The effect of molecular weight and crystallinity on the mechanical properties of injection moulded poly(aryl-ether-ether-ketone) resin[J]. *Polymer*, 1994, 35(1):110-116.
26. Jaekel D J, Macdonald D W, Kurtz S M. Characterization of PEEK biomaterials using the small punch test.[J]. *Journal of the Mechanical Behavior of Biomedical Materials*, 2011, 4(7):1275-82..
27. Chairperson C D S C. Fused deposition modeling with localized pre-deposition heating using forced air[M]// *Stochastic aspects of classical and quantum systems* . Springer-Verlag, 1985:1975-1975.
28. Anitha R, Arunachalam S, Radhakrishnan P. Critical parameters influencing the quality of prototypes in fused deposition modelling[J]. *Journal of Materials Processing Tech*, 2001, 118(1):385-388.
29. Fujihara K, Huang Z M, Ramakrishna S, Hamada H. Influence of processing conditions on bending property of continuous carbon fiber reinforced PEEK composites[J]. *Composites Science & Technology*, 2004, 64(16):2525-2534.
30. Grouve W J B, Warnet L L, Rietman B, Visser H A, Akkerman R. Optimization of the tape placement process parameters for carbon-PPS composites[J]. *Composites Part A: Applied Science and Manufacturing*, 2013, 50: 44-53.
31. Grouve W J B, Poel G V, Warnet L L, Akkerman R. On crystallisation and fracture toughness of poly(phenylene sulphide) under tape placement conditions[J]. *Plastics Rubber & Composites*, 2013, 42(7):282-288.
32. Grouve W J B, Warnet L, Akkerman R, Wijskamp S, Kok J S M. Weld Strength Assessment for Tape Placement[J]. *International Journal of Material Forming*, 2010, 3(1):707-710.
33. Parandoush P, Tucker L, Zhou C, Lin D. Laser assisted additive manufacturing of continuous fiber reinforced thermoplastic composites[J]. *Materials & Design*, 2017.